

PHASE COMPOSITION AND DISTRIBUTION OF ALLOYING ELEMENTS IN THE TRANSITION LAYER

Ya. S. Semenov,¹ S. K. Popova,²
and M. P. Lebedev¹

UDC 539.21 : 539.26 : 548.73 : 543.422.8 : 543.732

X-ray spectral and x-ray structural analyses and optical microscopy were used to study the chemical and phase compositions and the structure and morphology of alloying elements of the transition layer produced by gas-flame and plasma spraying on St. 3sp steels. It is shown that the structure and chemical and phase compositions of the transition layer depend significantly on the technological parameters, processing methods, and the chemical composition of the coating.

Key words: *chemical bonds, adhesion, brittle wear, transition layer, wear reduction.*

Introduction. Cleavage wear can occur during operation of parts remanufactured by low-temperature gas-flame or plasma methods and it is due to the following two major factors [1]: weak adhesion of the sprayed layer to the substrate due to small penetration into the substrate; cleavage due to operation of a part at a temperature below the critical cold brittleness temperature. This leads to the need to increase the degree of adhesion of the sprayed coating to the substrate and to raise its cold resistance, i.e., to create a coating–substrate transition layer that would have high adhesion and low cold brittleness temperature.

Gas-flame and plasma coatings, whose adhesion depends greatly on the distribution of alloying elements in the transition layer formed by the basic metal and coating, have been studied to evaluate the phase composition and distribution of chemical elements in the coating–substrate transition layer [2–5].

Because the transition layer is produced by different types of fusion, resulting in different degrees of adhesion of the sprayed layer to the substrate, it is necessary to determine the phase composition and distribution of alloying elements in the transition layer, first of all, the presence of chemical elements reducing the critical cold brittleness temperature. These data can be obtained using x-ray spectral and x-ray structural analyses and optical microscopy.

The purpose of the present work was to study the phase composition and distribution of chemical elements in the coating–substrate transition layer to optimize technological fusion parameters.

Technique of Producing the Transition Layer. Samples of sprayed coatings were produced and processed using Ni–Cr–B–Si (PGSR-4), Fe–C–Cr–V (KhVS), and Ni–Al powders, and Kh18N9T stainless steel powder.

The substrate was St. 3sp steel samples in the form of a 50 × 35 × 10 mm plate which was divided by cuts into six parts to avoid damage to the coating during subsequent machining. The starting powders had particle sizes of 60–100 μm.

Fusion was performed using a continuous-mode LOK-ZM CO₂ laser radiation with a wavelength of 10.6 μm in air. The total loss of the laser beam power due to reflection from the surface are approximately 17%. The laser radiation power was measured directly at the laser exit. Surface fusion was performed on a screw line with a constant step which provided continuity of the surface working at four power modes: 1.0, 1.2, 1.5, and 1.9 kW.

¹Presidium of the Yakutsk Research Center of the Siberian Division of the Russian Academy of Sciences, Yakutsk 677980; yansemenov@mail.ru. ²Institute of the Geology of Diamond and Precious Metals, Siberian Division of the Russian Academy of Sciences, Yakutsk 677891. Translated from *Prikladnaya Mekhanika i Tekhnicheskaya Fizika*, Vol. 50, No. 6, pp. 207–212, November–December, 2009. Original article submitted August 9, 2007; revision submitted December 27, 2008.

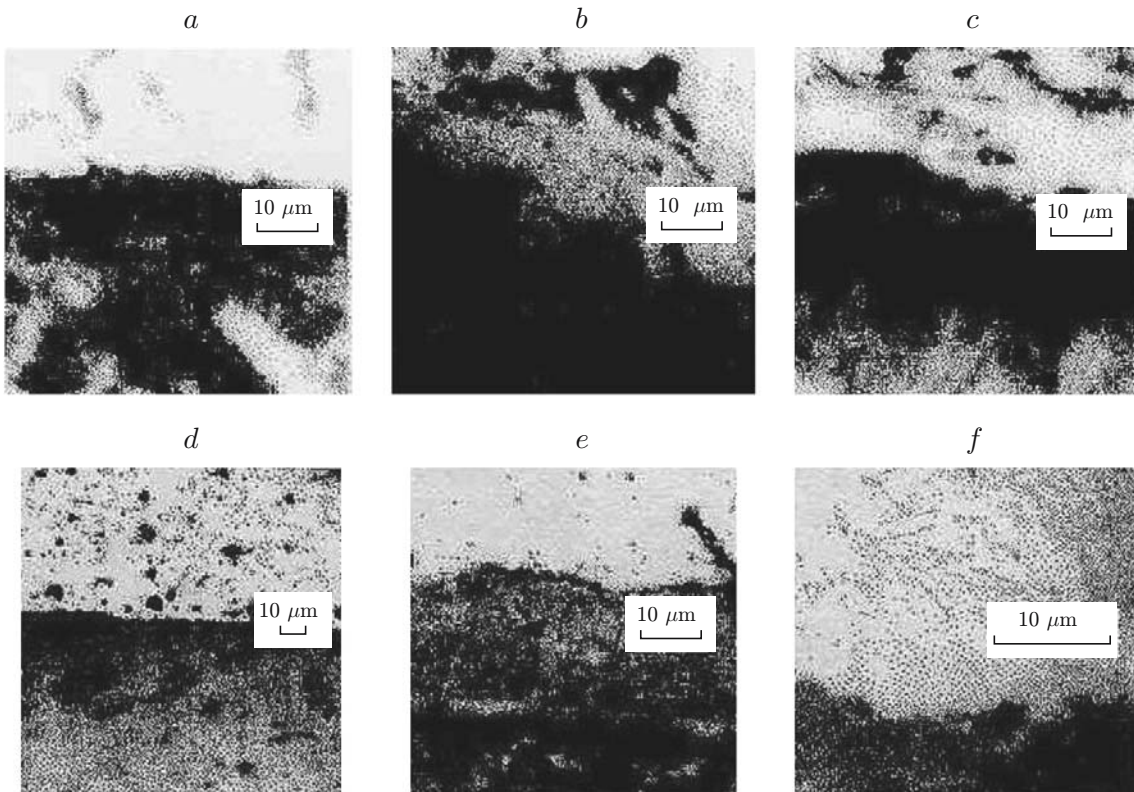


Fig. 1. Microstructure of the material in the fusion zone: (a–c) sprayed layers of thicknesses $H = 0.2$ (a), 0.5 (b), and 1.0 mm (c); (d–f) fused layer [unetched metallographic section (d), diffusion layer in the substrate (e), and diffusion layer in the sprayed coating (f)].

Experimental Results and Discussion. Stereometric metallographic analysis of the experimental results shows that an increase in the specific laser radiation energy during fusion leads to an increase in the mixing coefficient in the transition layer. In addition, as the mixing coefficient during fusion changes, the concentration of the hardening phases of the compositions studied structures changes by 20–35% (Fig. 1).

The hardening phases have different morphologies and both rounded and oval shapes. In some cases, they form a continuous net structure along crystallite boundaries, producing a sort of hardening framework, which is characteristic of alloyed layers produced with the use of slurry coatings.

To determine the effect of the structure of the transition layer, we studied samples with variously treated sprayed coatings for the contact wear resistance in disk on disk tests with sliding and loading at an air temperature of -15°C .

Before the tests on an SMTs-2 machine, the samples were finished to eliminate grinding traces. A roller of U8A tool steel (State Standard GOST-1435-74) (Rockwell hardness HRC = 65) was used as a counterbody. Wear of the coatings was measured (to within $\pm 2 \mu\text{m}$) after each 10^5 test cycles (approximately 5.5) using an UIM-23 microscope. Cleavage fracture along the transition layer was not observed.

It should be noted that laser penetration and the introduction of the chemical elements Ni, Cr, and V lead to a significant wear reduction and the formation of a transition layer with high adhesion preventing cleavage. As an example, Fig. 2 shows a curve of the wear of the coatings versus the number of test cycles $N = n \cdot 10^5$.

Chemical Composition of Coatings. The chemical composition of coatings was studied using a CAMEBAX electron-probe microanalyzer and a Si(Li)-solid-state detector with a primary electron beam energy of 10 keV, a current strength of 1 nA, a scanning area of $50 \times 50 \mu\text{m}$, and a time of 100 sec.

For quantitative analysis, samples of boron nitride (BN) and titanium (Ti) were used. The element distribution on the boundary between the Ni–Cr–Si–B coating and substrate was analyzed on metallographic cross sections. The morphology of the coating surface was studied using secondary-electron scanning electron microscopy (SEM).

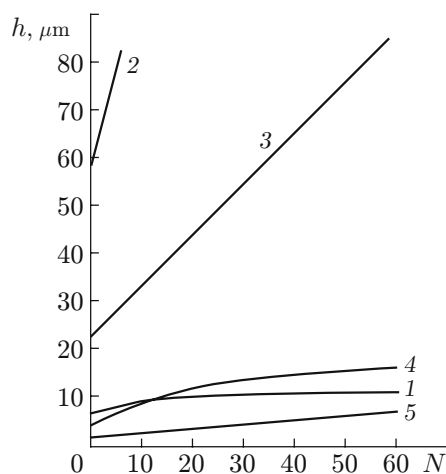


Fig. 2. Wear of coatings versus number of cycles of tests: 1) PGSR-4 with fusion; 2) KhVS without fusion; 3) Kh18N9T without fusion; 4) KhVS with fusion; 5) Kh18N9T with fusion.

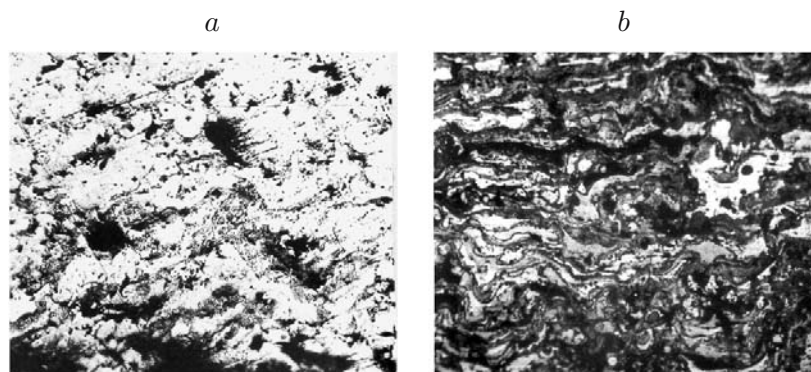


Fig. 3. Structure of coatings after gas-flame (a) and plasma (b) spraying.

Structure and Phase Composition of Coatings. The structure and phase composition of Ni-Cr-S-B coatings were determined on a DRON-3 x-ray diffractometer ($\text{CuK}\alpha$ radiation; $\lambda = 0.154178$ nm) with a graphite monochromator at scanning angles of $30\text{--}90^\circ$ and a scanning step of 0.05° .

An analysis of the Ni-Cr-S-B coatings was performed on $50 \times 35 \times 10$ mm samples whose flat side was preliminarily cut into six parts.

The coatings were obtained under the following conditions: voltage $U = 180$ V, current strength $J = 210$ A, distance to the spraying surface 100 mm, consumption of plasma-forming nitrogen 45 liters, consumption of the transporting gas 70 liters, powder particle size $80\text{--}100$ μm , powder flow rate 30 ml/min, and gas consumption for protection 90 liters. The coating thickness was $H = 0.2, 0.5,$ and 1.0 mm.

The coatings obtained under the same conditions (number of passages, thermal contribution) were similar in appearance: they were layered and dense and the metallographic sections had unfused initial particles of spherical shape of various structures.

The starting powder is a mixture of a nickel-based low-melting eutectic and a solid solution of boron, silicon, and chromium in nickel with carbide inclusions.

In gas-flame fusion, the coating 0.2 mm thick is porous and layered and therefore has weak adhesion to the substrate (Fig. 3a). The coating applied by plasma spraying has good adhesion due to the best mixing with the substrate and do not have pores and cleavages (Fig. 3b).

Coatings 0.5–0.6 mm thick, which are more interesting from a practical point of view, require additional treatment. The sprayed coatings preheated to a temperature of $300\text{--}400$ $^\circ\text{C}$ (without overheating) was fused using a propane-butane gas-flame burner.

TABLE 1

Phase Composition of Coatings

| Coating material | treatment mode | Interplane distance (d , Å) | Current strength | Phase |
|------------------|-----------------------|--------------------------------|------------------|---------------------------------|
| Ni-Cr-B-Si | Spraying | 2.018 | High | Ni |
| | | 1.362 | Low | Cr ₇ C ₃ |
| | | 1.491 | Low | CrB |
| | | 1.728 | Low | Cr ₇ C ₃ |
| | | 1.656 | Low | Ni ₂ Si |
| | | 1.978 | Moderate | Ni ₂ Si |
| Ni-Cr-B-Si | Laser fusion (mode 1) | 3.272 | Low | Fe ₂ B |
| | | 2.710 | Moderate | Fe ₂ B |
| | | 2.291 | Moderate | Fe ₂ B |
| | | 2.193 | High | Fe ₂ B |
| | | 2.009 | High | α-Fe |
| | | 1.792 | Moderate | Cr ₂₃ C ₆ |
| | | 1.316 | Low | Fe ₂ B |
| Ni-Cr-B-Si | Laser fusion (mode 2) | 1.454 | Low | Cr ₇ C ₃ |
| | | 1.416 | Low | Cr ₃ C ₂ |
| | | 1.366 | Low | Cr ₇ C ₃ |
| | | 1.789 | Low | Cr ₃ C ₂ |
| | | 1.812 | Low | Cr ₇ C ₃ |
| | | 1.954 | Moderate | Cr ₃ C ₂ |
| | | 2.002 | Moderate | α-Fe |
| Ni-Cr-B-Si | Laser fusion (mode 3) | 2.473 | Moderate | Cr ₃ C ₂ |
| | | 2.823 | High | α-Fe |
| | | 1.861 | Low | Cr ₃ C ₂ |
| | | 1.791 | Moderate | Cr ₂₃ C ₆ |
| Ni-Al | Spraying | 2.007 | High | Ni |
| | | 1.794 | Moderate | Ni ₃ Al |
| Ni-Al | Laser fusion (mode1) | 1.434 | Low | α-Fe |
| | | 2.002 | High | α-Fe |
| | | 2.210 | Moderate | α-Fe |

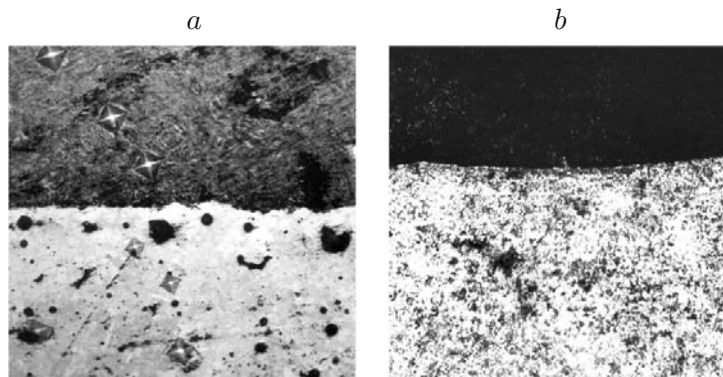


Fig. 4. Microstructure of the coatings fused by a gas burner (a) and plasma (b).

The microstructure of the fused coatings is shown in Fig. 4. It is evident that the coatings have dense fine-grained structure with no layering. Carbides and borides have the shape of platelets and grains of various shapes and sizes. The width of the diffusion zones L is insignificant (see Fig. 4). Metallographic analysis shows that the subsequent treatment allows one to considerably improve both the structure and the strength of adhesion of the coating to the substrate.

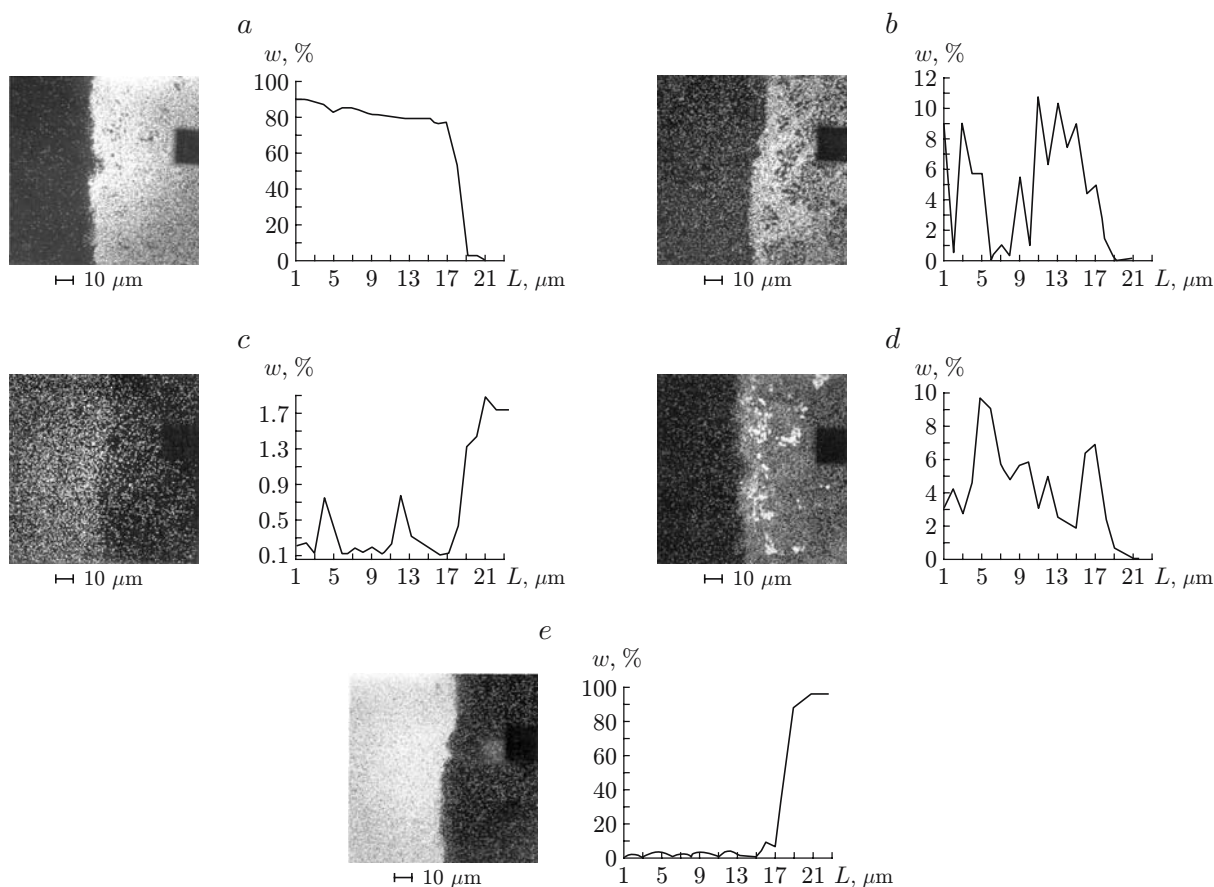


Fig. 5. Concentration of alloying elements in the sprayed coatings: nickel (a), silicon (b), manganese (c), chromium (d), and iron (e).

X-Ray Structural Analysis. To evaluate the effect of gas-flame fusion on the phase composition, we performed x-ray structural analysis, which shows that the sprayed coating consists of a Ni based solid solution with the CrB and Cr₇C₃ hardening phases. Silicon compounds were not found in the fused samples. After fusion, the Fe₂B hardening phase appears, which indicates the removal of Fe from the substrate (see Table 1).

X-Ray Spectral Analysis. X-ray spectral analysis makes it possible to estimate the chemical composition of the coating formed and the distribution of alloying elements in it. Investigation of the chemical composition of the sprayed coatings shows that the chemical elements, in particular, chromium and silicon are distributed nonuniformly (Fig. 5). After fusion, the curves of $w(L)$ for chromium and silicon are similar to the curves for the unfused layer before the diffusion zone, notwithstanding that the structure of the coatings changes greatly. The width of the diffusion zone increases by a factor of four, the nickel and iron concentrations in the zone vary uniformly, and the chromium and silicon concentration decrease gradually. The presence of a diffusion zone with a uniform distribution of elements indicates enhanced adhesion of the sprayed layer to the substrate.

Thus, x-ray structural and x-ray spectral studies allow one to determine the phase and chemical compositions of the transition layer and correct the technological fusion modes to increase adhesive properties.

After a certain modification, this technique can be applied to nanomaterials using a scanning tunnel microscope.

This work was supported by the Russian Foundation for Basic Research (Grant No. 06-08-96016 Dal'nii Vostok).

REFERENCES

1. B. K. Barakhtin, M. P. Lebedev, P. P. Petrov, and V. V. Makarov, *Optimization of the Internal Structure of Materials for Operation under Extreme Conditions* [in Russian], Akademiya, Moscow (2000).
2. A. G. Grigoryants, *Principles of Laser Processing of Materials* [in Russian], Mashinostroenie, Moscow (1989).
3. A. V. Chichinadze (ed.), *Friction and Wear of Frictional Materials* [in Russian], Nauka, Moscow (1977).
4. K. I. Krylov, V. T. Prokopenko, and A. S. Mitrofanov, *Using Lasers in Mechanical Engineering and Instrument Making* [in Russian], Mashinostroenie, Leningrad (1978).
5. V. M. Buznik, M. P. Lebedev, and Ya. S. Semenov, "On the starting period of friction couples under conditions of the Far North," *Trenie Iznos*, **26**, No. 2, 191–196 (2005).